第 43 卷 第 2 期/2023 年 1 月/光学学报 研究论文

光学学报

大功率LED纳米银烧结界面热阻和发光性能

梁仁璞[1,2]，刘佳欣[3]，赵九洲[4]，彭洋[4]，王新中[2**]，杨军[1*]

[1]电子科技大学（深圳）高等研究院，广东 深圳 518110；

[2]深圳信息职业技术学院信息技术研究所，广东 深圳 518172；

[3]华中科技大学机械科学与工程学院，湖北 武汉 430074；

[4]华中科技大学航空航天学院，湖北 武汉 430074

摘要 利用纳米银烧结工艺制备大功率LED，重点探究了纳米银键合层的界面热阻及器件发光性能。通过将纳米银膏在不同温度下烧结，系统地研究了烧结温度对纳米银烧结后电阻率及接头剪切强度的影响，并分析了烧结后银膏的晶体结构及接头断口微观形貌。结果表明，接头键合强度和银膜导电率均随纳米银烧结温度的升高而增大。实验中还对比分析了纳米银烧结LED和传统锡银铜（SAC305）焊膏封装LED的界面热阻、结温以及发光性能。与纳米银烧结LED样品相比，传统焊膏封装LED的界面热阻和结温分别提高了8.9%和29.6%，说明纳米银键合层拥有更好的导热性并可及时为芯片散热降温。此外，通过高温老化实验，深入探讨了不同焊膏烧结LED的界面热阻及发光效率变化。实验表明，经过100 ℃下点亮500 h，纳米银和传统焊膏烧结LED样品的总热阻分别增大了0.03 K/W和4.28 K/W，但纳米银键合层界面热阻比老化前有所降低，同时纳米银烧结LED样品在不同电流下的发光效率始终高于传统焊膏封装LED样品。

关键词 材料；大功率LED；光热性能；发光稳定性；纳米银烧结；界面热阻

中图分类号 O436 **文献标志码** A **DOI**：10.3788/AOS221116

1 引 言

发光二极管（LED）是基于p-n结电致发光原理的半导体发光器件，具有光效高、寿命长、环保节能、结构紧凑等优点，已被广泛应用于照明和背光显示领域，如道路照明、室内照明、汽车大灯、电视背光、手机闪光灯等[1-4]。随着人们在照明和显示领域的需求日益增加，LED技术向着大功率和高密度方向发展，发光性能也成为一个重要的衡量指标。研究表明，通过内嵌式陶瓷电路板技术和掺杂金属及其他化学复合物质的技术能改善LED的发光性能[5-8]，但LED的散热对发光性能的影响是不可忽视的。LED电光转换效率不足60%，导致部分输入电能转换为热量，且随着LED输入功率的增大，LED芯片产生的热量不断升高。过高的热量将导致LED产生温升效应，使得芯片结温升高，一方面使LED性能降低（如发光效率降低、波长红移等），另一方面将在LED器件内部产生热应力，引发一系列可靠性问题（如使用寿命短、色温变化大等）[9-11]。因此，为了避免高温对LED芯片的热损耗，有必要增强LED散热性能，从而提高大功率LED发光性能。

为了获得LED封装模块，需要将LED芯片贴装或固定于封装基板上（固晶过程），封装基板利用材料本身的高热导率，将热量从LED芯片（热源）导出，实现与外界环境的热交换。值得注意的是，在LED芯片热量向封装基板传导过程中，芯片与封装基板间的键合层（固晶材料）决定着热量传导效率和能力。目前，常用的LED固晶材料主要包括LED导电胶、锡基焊料、纳米焊膏等[12-15]。导电胶作为一种多组分复合型功能材料，主要由基体树脂、固化剂、导电填料等组成，其中基体树脂通过交联反应形成分子骨架网状结构，使得导电填料连接形成导电通路，为LED提供粘附和导电功能。但是，导电胶中基体树脂的耐热性和导热性较差，导致高热量下导电胶出现老化和炭化问题，这就使其很难满足大功率LED封装需求[16]。针对这一问题，锡基焊料被用于LED芯片贴装，包括Cu-Sn、Sn-Bi和Au-Sn等，体现出可焊性良好、性价比高、熔点低等优势。但是，Cu-Sn焊料难以耐受高温，存在电迁移问题；Sn-Bi焊料导电性差，脆性相对较大；Au-Sn焊料设备要求高，工艺温度高，易损伤LED芯片[17-19]。近年来，由于纳米材料的小尺寸效应，金属纳米颗粒（铜、银等）的熔点随着纳米颗粒尺寸的减小而降低，从而能够

收稿日期：2022-05-13；**修回日期**：2022-07-08；**录用日期**：2022-07-21；**网络首发日期**：2022-07-30

基金项目：中国博士后科学基金（2021M700692）、深圳市科技计划项目（JSGG20201102152403008）、深圳市科技计划项目（JSGG20210802154213040）、创新强校项目（PT2020C002）

通信作者：*junyang@uestc.edu.cn；**xzwang868@163.com

在远低于块体熔点的温度下烧结成型。同时，纳米材料经烧结后能在较高温度下长期稳定工作，很好地满足了“低温烧结、高温服役”的需求，使得纳米焊膏已经被用于大功率器件封装[20-23]。虽然纳米铜焊膏导电导热性能好、成本低，但是铜纳米颗粒在空气中极易被氧化，表面氧化物会降低焊膏的表面活性和扩散系数以及提高键合温度，严重影响纳米铜焊膏的键合性能[24-26]。与其他焊料相比，纳米银焊膏具有键合温度低、键合面要求低、键合层熔点高等优点，且导电导热性强、易储存以及操作简便，可满足大功率LED封装对散热和长期服役的封装需求[27]，同时能很好地提高LED的出光效率以及光提取效率[28-29]。虽然纳米银焊膏已经被用于大功率LED封装，但是纳米银烧结界面热阻和长期可靠性有待进一步研究，而针对纳米焊膏键合层的散热性能和稳定性的研究对于纳米银烧结大功率LED具有十分重要的意义。

本文将纳米银焊膏用于大功率LED封装，系统研究了大功率LED中纳米银烧结界面热阻和发光性能。实验过程中，分析了不同烧结温度下纳米银键合层的电阻率、键合强度、微观形貌等，对比研究了纳米银焊膏和普通锡银铜焊膏烧结LED的热阻、结温以及光学性能，探讨了老化条件下不同焊膏烧结LED的界面热阻和发光效率的变化规律。

2 实　　验

2.1 纳米银烧结大功率LED

图1为纳米银烧结大功率LED的封装工艺流程图。本实验中使用的纳米银膏为ADGE-02无压烧结银膏；所使用的芯片为含直接电镀铜（DPC）陶瓷基板的垂直封装型大功率蓝光LED芯片，功率为1 W；所使用的封装基板为六角铜基板。首先，使用

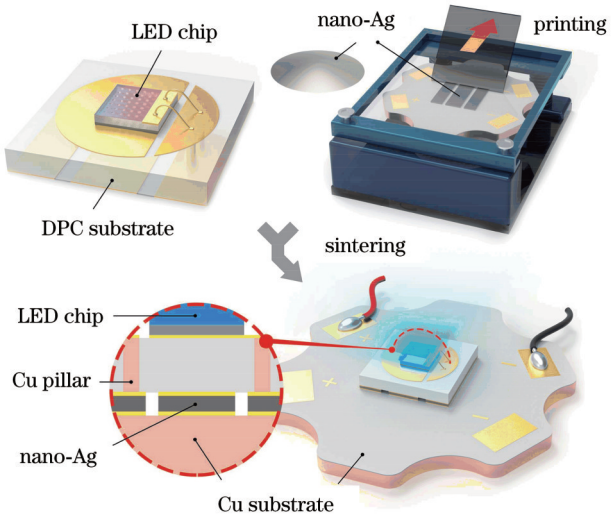

图1　纳米银烧结大功率LED的封装工艺流程

Fig. 1　Packaging process of high-power LED with nano-silver sintering

丙酮和无水乙醇溶液超声清洗芯片和封装基板，以去除其金属层表面油污和杂质；其次，采用丝网印刷技术在六角铜基板表面涂覆纳米银膏，印刷厚度为50 μm；然后，将含芯片的DPC陶瓷基板背部金属焊接层与铜基板线路层对准并水平放置；最后，将LED整体结构放到鼓风烘箱中进行烧结。烧结时先在120 ℃保温10 min，以充分挥发其内部有机溶剂，接着在200 ℃温度下烧结60 min，得到封装完毕的大功率LED器件。

为了探究不同烧结温度对纳米银膏电阻率的影响，将纳米银膏涂覆在石英玻璃表面，分别在180、200、220、240 ℃下进行低温烧结。同时，利用纳米银膏对镀银铜片（10 mm×10 mm×2 mm和3 mm×3 mm×2 mm）进行低温键合，测试不同键合温度下接头的力学性能。为了对比纳米银烧结LED器件的界面热阻及封装可靠性，采用传统锡银铜（SAC305）焊膏在相同工艺下封装LED，其焊接过程在普通回流炉内完成。

2.2 性能表征

采用台阶仪（ET4000 Series）测试不同温度下烧结的纳米银薄膜厚度，并采用四探针测试仪（Probes Tech RST-8）测试烧结银膜的方块电阻。利用推拉力测试机（Dage-4000Plus Bond）测试铜-铜键合接头的剪切强度。利用X射线衍射仪（X’Pert3 PRO MRD）检测烧结后纳米银焊膏的晶体结构。采用扫描电子显微镜（SEM；Nova Nano SEM 450，FEI）观察接头断口形貌。通过超景深三维显微镜（KEYENCE，VHX-1000，Japan）观察大功率LED横截面结构，并利用SEM观察键合层银膏截面形貌。采用红外热像仪（FLIR，E63，USA）测试大功率LED表面工作温度。通过热阻测试仪（T3ster-Master，Mentor Graphics）测试LED器件在不同驱动电流下的结温变化和结构热阻，其中测试电流为1 mA，温控模块为干式温控仪，热平衡时间为75 s。采用LED自动温控光电分析测量系统（杭州远方光电信息股份有限公司，ATA-1000）测试LED样品的发射光谱和光功率。

3 结果与讨论

3.1 纳米银膏烧结性能表征

将测试得到的烧结银膜方块电阻和银膜厚度相乘，可得到不同温度下烧结后纳米银膏的电阻率，结果如图2（a）所示。随着烧结温度从180 ℃升到240 ℃，纳米银薄膜的厚度分别为47、43、42、39 μm，其烧结后电阻率逐渐降低，分别为8.74、6.23、4.46和4.02 μΩ·cm。较高的温度会带来较大的烧结驱动力，从而加速纳米颗粒的烧结和扩散，这有利于晶粒的形成[30]。因此，高温下烧结的纳米银结构更加致密，电阻率更小。在240 ℃烧结后，纳米银电阻率与金属银电阻率的理论值接近，表明此时烧结较为完全。图2（b）

所示为不同键合温度下铜-铜接头的剪切强度值。当键合温度从180 ℃升到240 ℃时，接头剪切强度值逐渐增大，从16.7 MPa升高到21.2 MPa。由此可见，纳米银烧结温度越高，其导电性能和力学性能越好。图2(c)为纳米银膏在200 ℃烧结后的XRD图，图中显示出4个衍射峰，分别对应银晶体的(111)、(200)、(220)和(311)晶面。图谱中无其他杂质峰，表明在200 ℃烧结后，纳米银膏内部的有机溶剂完全分解并形成了银单质，展现出其优良的导电、导热性能。图2(d)展示了键合温度为200 ℃时接头的断面图，从该断面图中可以明显看到纳米银颗粒的韧性断裂形貌。颗粒在高温下烧结熔化并形成烧结颈，在推力的作用下，颗粒被拉长直至发生韧性断裂。为了降低LED封装时高温给芯片带来的热应力，本实验设定烧结温度为200 ℃(比SAC305的烧结温度低约50 ℃)，并对该器件进行热学、光学及高温可靠性分析。

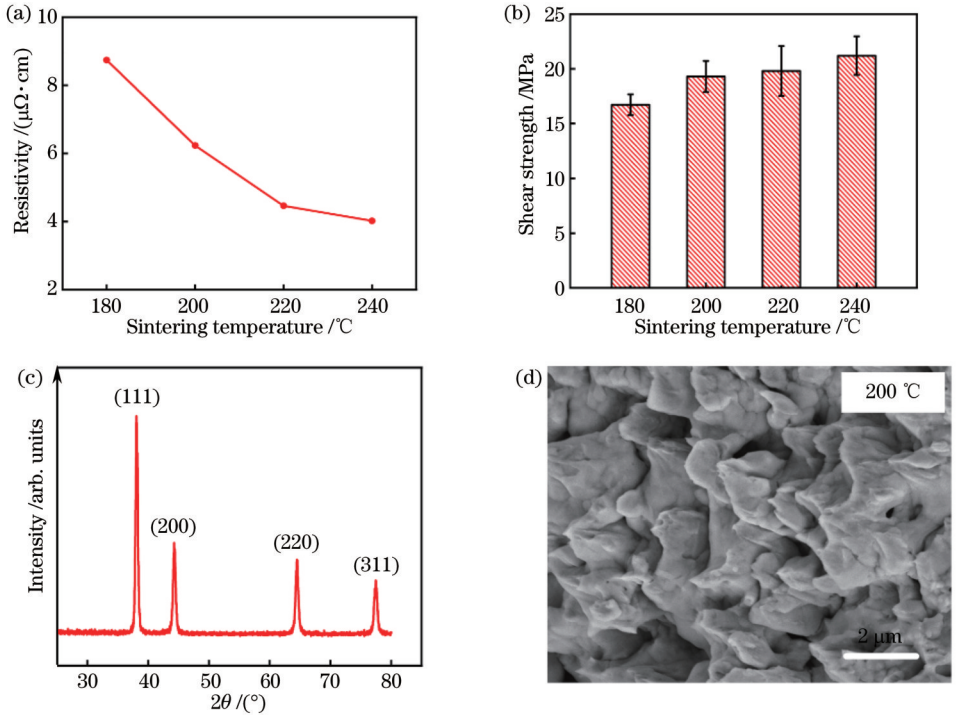

图2　不同烧结温度下的银膏性能。(a)电阻率；(b)剪切强度；(c) 200 ℃烧结后纳米银焊膏的XRD图；(d)键合层断口形貌

Fig. 2　Properties of Ag paste under various sintering temperatures. (a) Electrical resistivity; (b) shear strength; (c) XRD image of nano-silver paste after sintering at 200 ℃; (d) fracture morphology of bonding layer

图3(a)所示为封装后LED模组的横截面图。可以看出，该大功率LED芯片为垂直封装结构，模组从上到下依次为芯片、金属层、AlN陶瓷基板、金属焊盘、纳米银键合层和六角铜基板。图3(b)为图3(a)红框区域的放大图，即纳米银键合层的扫描电子显微镜(SEM)截面图。可以看到，键合层结构致密，内部无孔洞和裂纹产生。同时，纳米银层与上下基板的键合界面清晰，界面处无细纹等缺陷，形成了较好的冶金结合，表明纳米银膏烧结后的LED模组具有良好的封装质量。

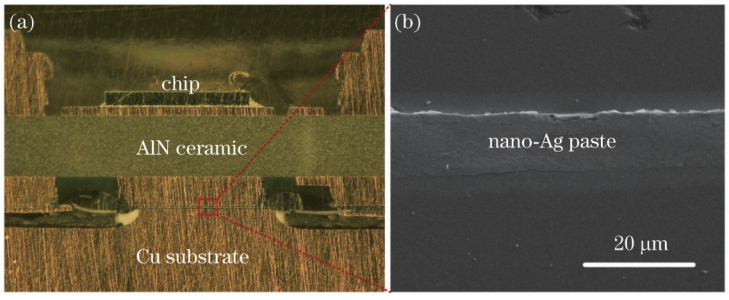

图3　LED模组横截面图。(a)光镜下LED截面图；(b)纳米银键合层SEM截面图

Fig. 3　Cross-sectional images of LED module. (a) Cross-section of LED under optical microscope; (b) SEM image of nano-silver bonding layer

3.2　纳米银烧结 LED 的热学和光学性能

为了探究 LED 封装样品键合层对器件热学及光学性能的影响，对纳米银膏和 SAC305 焊膏烧结后的 LED 模组进行测试。图 4(a)、(b)分别为纳米银焊膏和 SAC305 烧结 LED 在驱动电流为 350 mA 时的热像图，其中纳米银膏烧结 LED 样品的工作温度为 26.7 ℃，比 SAC305 焊膏封装 LED 样品的工作温度(34.6 ℃)低 22.8%。图 4(c)所示为不同驱动电流下，点亮 5 min 后 LED 的工作温度。可以看到，不同焊膏封装后 LED 样品的表面温度均随驱动电流的增大而缓慢升高。当驱动电流以 100 mA 为间隔从 200 mA 上升到 700 mA 时，纳米银烧结 LED 样品的工作温度分别为 26.5、26.5、26.6、26.9、27.5、28.5 ℃，而 SAC305 焊膏封装 LED 样品的工作温度分别为 32.7、34.0、34.6、34.5、35.1、35.3 ℃。在相同的驱动电流下，两种样品表面的温差分别为 6.2、7.5、8.0、7.6、7.6、6.8 ℃，表明与传统锡膏相比，纳米银具有更低的界面热阻，可提高 LED 器件的散热性能，并实现更低的工作温度。LED 样品在驱动电流下达到热平衡，并在小测试电流下降温至和环境温度达到新的热平衡状态，采用热阻测试仪记录被测 LED 的正向电压，并通过温度系数的计算公式将该 LED 的电压随时间的变化关系转换为相应的温度随时间变化的关系，得到瞬态温度响应曲线(结温变化曲线)，该被测 LED 的结温即为环境温度与测试结温变化之和。图 4(d)展示了驱动电流为 350 mA 时两种 LED 的结温变化，纳米银烧结 LED 样品的结温变化为 2.33 ℃，比 SAC305 焊膏封装 LED 样品的结温变化(4.25 ℃)低 45.2%。

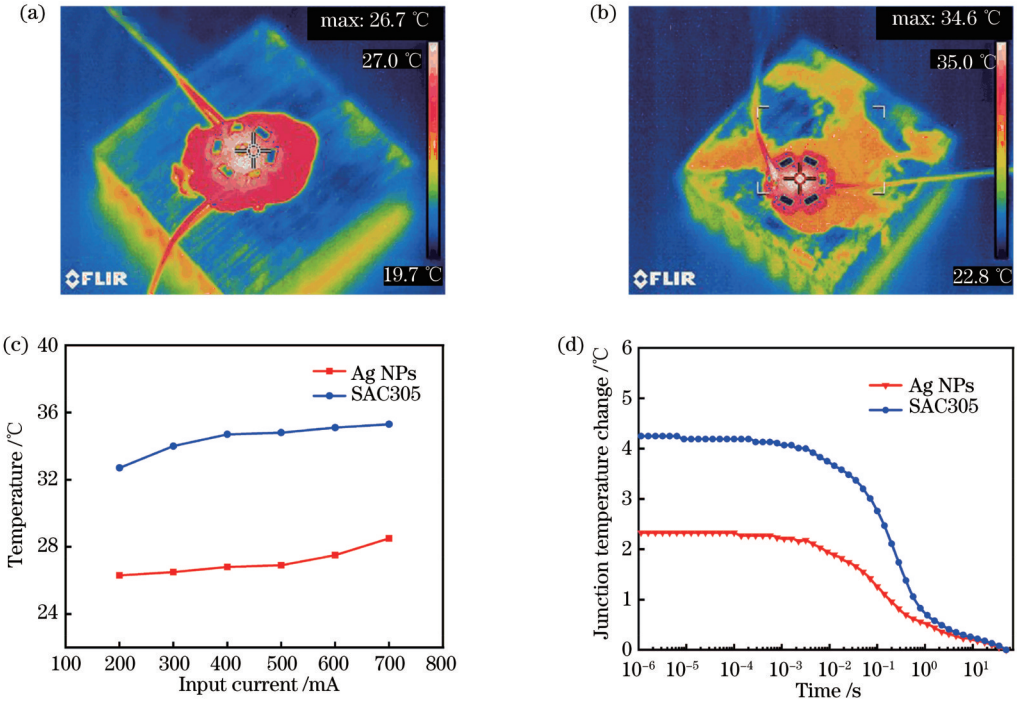

图 4　纳米银焊膏(Ag NPs)和锡银铜焊膏(SAC305)烧结 LED 的热学性能。(a)纳米银焊膏烧结样品在 350 mA 时热像图片；(b)SAC305 焊膏烧结样品在 350 mA 时热像图片；(c)不同电流下 LED 工作温度；(d)电流为 350 mA 时 LED 结温变化

Fig. 4　Thermal properties of sintered LED with Ag NPs and SAC305. (a) Thermal image of Ag NPs sintered LED at 350 mA; (b) thermal image of SAC305 sintered LED at 350 mA; (c) working temperatures of LED under various currents; (d) junction temperature change of LED at 350 mA

图 5(a)所示为 350 mA 驱动电流下不同焊膏烧结后 LED 的微分热阻。基于 T3Ster 热阻测试仪原理及传热理论，LED 芯片与铜基板间的热阻可表示为

$$R_{\mathrm{th}}=\frac{T_1-T_2}{P_1-P_2},\tag{1}$$

式中：T_1、T_2分别表示 LED 芯片和六角铜基板底面的温度；P_1、P_2分别表示流过 LED 芯片和铜基板间的热量。由图 5(a)可知，SAC305 封装 LED 样品的总热阻为 8.26 K/W，比纳米银烧结 LED 样品的总热阻 7.25 K/W 高 1.01 K/W。微分热阻曲线图中每个波峰之间区域代表着相对应 LED 结构的热阻值，波峰将曲线从左至右划分为 5 个区域，分别对应 LED 芯片、银胶、AlN 陶瓷基板、键合层和六角铜基板的电阻值。其中，两种样品的键合层分别为 SAC305 焊膏和纳米银膏，界面热阻值分别为 0.73 K/W 和 0.67 K/W，SAC305 焊膏界面热阻比纳米银膏界面热阻高 8.9%，表明纳米银的导热性要优于传统锡膏。图 5(b)所示为两种 LED 样品的积分热阻曲线，它是通过对微分热阻函数曲线做积分运算得到的，表征积分热容与热阻的关系。积分热阻结构函数由平滑段和斜坡段组成，

其中每个平滑段与微分曲线对应，表征LED各个结构的界面热阻。利用积分热阻曲线可更直观地对比每个结构的热阻值，从图5(b)所示的曲线可以看出，纳米银烧结LED样品的总热阻和各结构界面热阻均比SAC305烧结样品有所降低，表明纳米银的高热导率有助于LED整体散热，使芯片热量更快耗散，以减少每个界面间热量的聚集。

通过改变热阻测试仪中加热电流大小来测试不同电流下两种LED样品的结温变化，结果如图6(a)所示。可以看到，随着加热电流的增大，LED结温变化逐渐升高。当加热电流从200 mA增大到700 mA时，纳米银烧结LED样品的结温变化从1.67 ℃增大到6.79 ℃，SAC305封装LED样品的结温变化从2.06 ℃提高到8.80 ℃，SAC305封装LED样品的结温始终高于纳米银烧结LED样品。当加热电流为700 mA时，SAC305封装LED样品结温变化比纳米银烧结样品高29.6%。图6(b)、(c)分别为纳米银和SAC305烧结LED在350 mA电流下的点亮实物图，可见两个大功率蓝光LED芯片颜色均匀、发光稳定。以上结果表明，纳米银较低的界面热阻有利于降低芯片温度，从而得到更低的结温值，这有助于延长LED器件寿命，提高其可靠性。

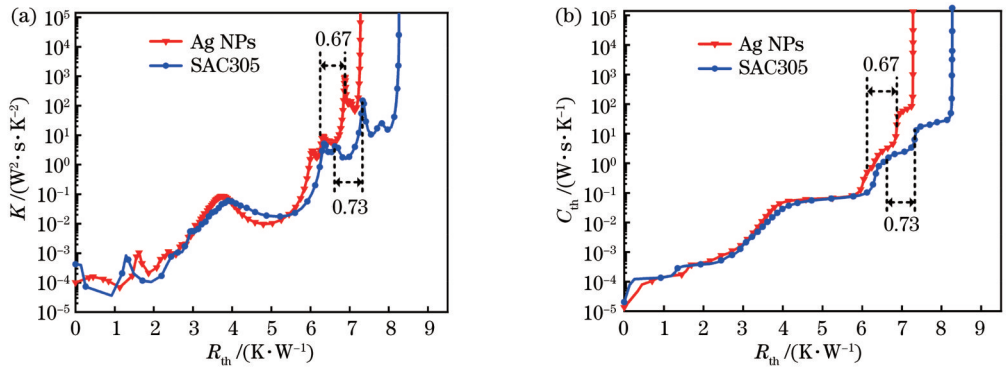

图5 不同焊膏烧结LED的热阻。(a)微分热阻；(b)积分热阻

Fig. 5 Thermal resistance of sintered LED with different pastes. (a) Differential thermal resistance; (b) integral thermal resistance

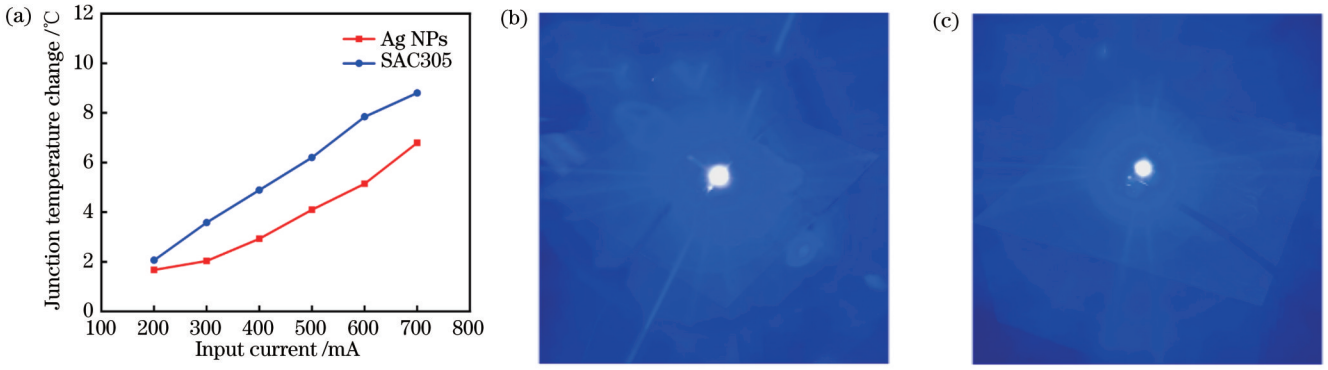

图6 LED在不同驱动电流下的结温变化和点亮图。(a)结温变化；(b)纳米银焊膏烧结LED实物图；(c)锡银铜焊膏烧结LED实物图

Fig. 6 Junction temperature change of LED under different driving currents and lighting pictures. (a) Junction temperature change; (b) picture of LED sintered with Ag NPs; (c) picture of LED sintered with SAC305

不同电流下LED的光学性能不同[31]，因此测量了LED样品在不同电流下的光谱图，结果如图7所示。随着电流从200 mA增大到1200 mA，两种LED的光谱强度均逐渐增大。对比发现，相同驱动电流下纳米银烧结LED的光谱强度始终高于SAC305封装LED样品，这可能是因为纳米银具有良好的导热性，使总功率更多地转化为光功率，从而提升LED的光谱强度和光效。

3.3 纳米银封装LED的发光稳定性

为了探究不同键合层对大功率LED可靠性的影响，将两种LED放入烘箱中进行高温老化测试，老化温度为100 ℃，老化时间为500 h，老化时驱动电流为350 mA。图8(a)所示为老化后两种LED微分热阻的变化曲线，与老化前[图5(a)]相比，纳米银烧结LED样品的总热阻从7.25 K/W增大到7.28 K/W，SAC305封装LED样品的总热阻从8.26 K/W增大到12.54 K/W，两种LED的总热阻分别比老化前增加了0.03 K/W和4.28 K/W。同时，纳米银和SAC305封装样品的键合层界面热阻分别变为0.56 K/W和1.04 K/W，老化后SAC305焊膏封装样品的界面热阻比纳米银膏封装样品的界面热阻高85.7%。上述结果表明：普通锡膏的高温可靠性不如纳米银膏，在长期高温工作中，锡膏内部可能出现扩散和迁移，从而产生

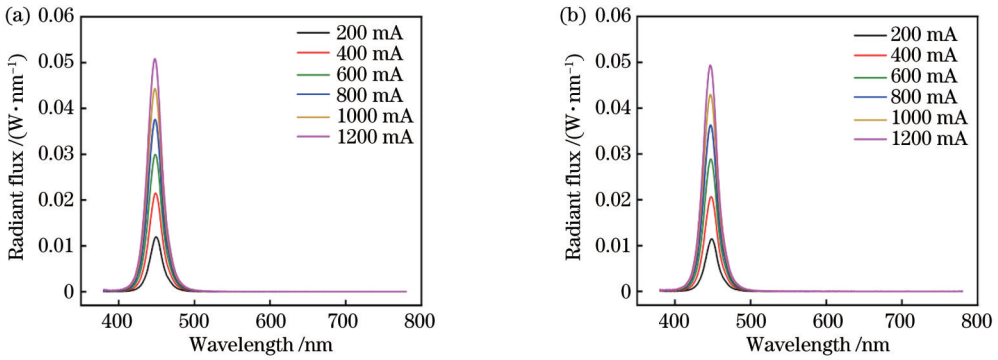

图 7　LED 在不同电流下的光谱图。(a)纳米银焊膏;(b)锡银铜焊膏

Fig. 7　Spectra of sintered LEDs at different currents. (a) Ag NPs; (b) SAC

Kirkendall 空洞,降低界面热阻;纳米银膏老化后界面热阻比老化前降低,这说明其本身化学性质稳定并可耐受高温。同时,在高温下,随着银纳米颗粒的深入烧结,其颗粒继续长大形成烧结颈,使得烧结更加充分,热导率提升。图 8(b)所示为高温老化 500 h 后两种 LED 样品的结温变化曲线,纳米银和 SAC305 封装 LED 样品的结温变化分别为 4.33 ℃和 6.41 ℃,纳米银烧结 LED 样品的结温变化比 SAC305 封装 LED 样品低 32.4%,这是因为老化后纳米银具有更低的界面热阻,可提升其散热性能并降低芯片结温。

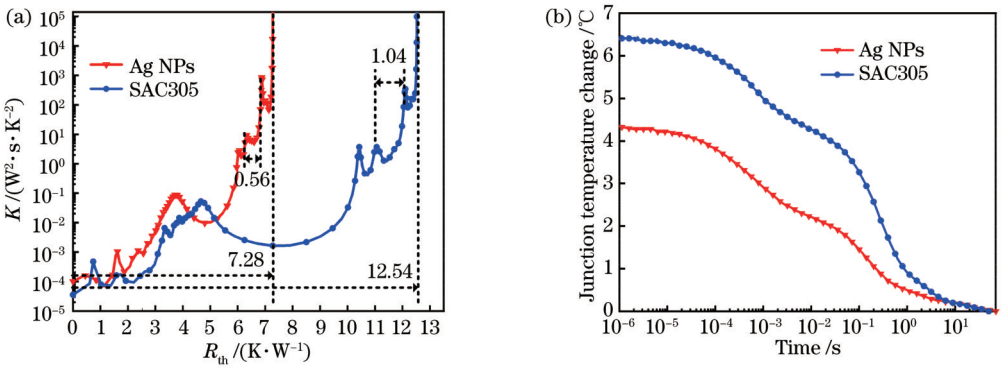

图 8　不同焊膏烧结 LED 在 100 ℃下点亮 500 h 后的热学性能。(a)热阻;(b)结温变化

Fig. 8　Thermal performance of LED sintered with different solder pastes after operated at 100 ℃ for 500 h. (a) Thermal resistance; (b) junction temperature change

图 9 为不同焊膏烧结 LED 在高温老化 500 h 后的光效(光功率与总功率的比值)图。随着驱动电流的增大,两种 LED 的光效逐渐降低,这是因为较大的电流会带来较大的热量,使得芯片升温,热功率所占比例增大,因此光效降低。由图 9 可知,纳米银烧结 LED 的光效始终高于 SAC305 封装 LED。当电流为 700 mA 时,纳米银烧结 LED 的光效为 41.1%,比 SAC305 封装 LED 样品的 39.6% 高 1.5%,这表明纳米银烧结 LED 样品因其较好的导热性而具有更高的光功率。

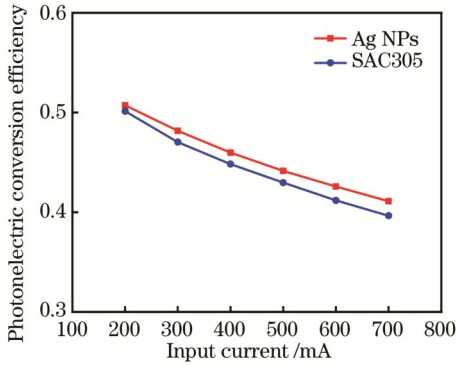

图 9　不同焊膏烧结 LED 在 100 ℃下点亮 500 h 后的光电转换效率

Fig. 9　Photoelectric conversion efficiency of LED sintered with different solder pastes after operated at 100 ℃ for 500 h

4　结　　论

利用纳米银烧结技术制备了大功率 LED 器件,并重点探究了键合层界面热阻及其发光性能。实验结果表明,随着烧结温度的升高,纳米银的电阻率不断降低,铜-铜接头的键合强度逐渐升高。当烧结温度为 240 ℃时,烧结银膜电阻率为 4.02 μΩ·cm,接头剪切强度为 21.2 MPa,断口呈韧性断裂。纳米银烧结 LED 键合层界面致密无裂纹,形成了良好的冶金结合。利用相同工艺制备了由传统锡银铜焊膏封装的 LED,并对比两种焊膏烧结 LED 的界面热阻、结温以及光学性

能。纳米银膏烧结LED样品比SAC305焊膏烧结样品具有更低的工作温度和总热阻，而SAC305焊膏界面热阻比纳米银膏高8.9%，表明纳米银具有更高的导热率和更好的散热性能。将两种LED样品在100 ℃进行500 h高温可靠性实验，实验结果表明，纳米银和SAC305封装LED样品的总热阻分别增大了0.03 K/W和4.28 K/W，但纳米银键合层界面热阻比老化前降低，可能是因为经高温老化过程后烧结更加充分，从而导致热导率提升。此外，不同电流下老化后纳米银烧结LED样品的光效始终高于SAC305封装LED样品。

参 考 文 献

[1] Schubert E F, Kim J K. Solid-state light sources getting smart [J]. Science, 2005, 308(5726): 1274-1278.

[2] Luo X B, Hu R, Liu S, et al. Heat and fluid flow in high-power LED packaging and applications[J]. Progress in Energy and Combustion Science, 2016, 56: 1-32.

[3] Peng Y, Li R X, Wang S M, et al. Luminous properties and thermal reliability of screen-printed phosphor-in-glass-based white light-emitting diodes[J]. IEEE Transactions on Electron Devices, 2017, 64(3): 1114-1119.

[4] 李晋闽, 刘志强, 魏同波, 等. 中国半导体照明发展综述[J]. 光学学报, 2021, 41(1): 0116002.
Li J M, Liu Z Q, Wei T B, et al. Development summary of semiconductor lighting in China[J]. Acta Optica Sinica, 2021, 41(1): 0116002.

[5] 王哲, 王永通, 刘佳欣, 等. 内嵌陶瓷电路板的PCB基板制备及其LED封装性能[J]. 发光学报, 2022,43(7):1139-1146.
Wang Z, Wang Y T, Liu J X, et al. Preparation of PCB Substrate embedded with ceramic circuit board and performance of LED packaging[J]. Chinese Journal of Luminescence, 2022, 43(7):1139-1146.

[6] 王晓琦, 王聪. Cu掺杂Zn-In-S/ZnS核/壳量子点白光LED壳层厚度对其发光性能的影响[J]. 激光与光电子学进展, 2021, 58(17): 1723003.
Wang X Q, Wang C. Influence of shell thickness on luminescent properties of Cu-doped Zn-In-S/ZnS core/shell quantum dots WLEDs[J]. Laser & Optoelectronics Progress, 2021, 58(17): 1723003.

[7] 刘源, 黄友强, 赵英杰, 等. 掺杂型二维材料发光性能研究进展[J]. 激光与光电子学进展, 2021, 58(15): 1516014.
Liu Y, Huang Y Q, Zhao Y J, et al. Luminescence properties of doped two-dimensional materials[J]. Laser & Optoelectronics Progress, 2021, 58(15): 1516014.

[8] Mou Y, Yu Z K, Lei Z Y, et al. Enhancing opto-thermal performances of white laser lighting by high reflective phosphor converter[J]. Journal of Alloys and Compounds, 2022, 918: 165637.

[9] Zhang K, Xiao G D, Zeng Z M, et al. A novel thermally conductive transparent die attach adhesive for high performance LEDs[J]. Materials Letters, 2019, 235: 216-219.

[10] 彭洋, 陈明祥, 罗小兵. 深紫外LED封装技术现状与展望[J]. 发光学报, 2021, 42(4): 542-559.
Peng Y, Chen M X, Luo X B. Status and perspectives of deep ultraviolet LED packaging technology[J]. Chinese Journal of Luminescence, 2021, 42(4): 542-559.

[11] 杨呈祥, 李欣, 孔亚飞, 等. 纳米银焊膏封装大功率COB LED模块的性能研究[J]. 发光学报, 2016, 37(1): 94-99.
Yang C X, Li X, Kong Y F, et al. High power COB LED modules attached by nanosilver paste[J]. Chinese Journal of Luminescence, 2016, 37(1): 94-99.

[12] 张保坦, 孙蓉, 汪正平. LED芯片键合材料研究述评[J]. 集成技术, 2014, 3(6): 1-7.
Zhang B T, Sun R, Wang Z P. LED Die bonding materials[J]. Journal of Integration Technology, 2014, 3(6): 1-7.

[13] Chen C J, Chen C M, Horng R H, et al. Thermal management and interfacial properties in high-power GaN-based light-emitting diodes employing diamond-added Sn-3 wt.% Ag-0.5 wt.% Cu solder as a die-attach material[J]. Journal of Electronic Materials, 2010, 39(12): 2618-2626.

[14] Cheng L C, Chen C M, Chen M G, et al. A high-temperature die-bonding structure fabricated at low temperature for light-emitting diodes[J]. IEEE Electron Device Letters, 2015, 36(8): 835-837.

[15] Jiang C S, Fan J J, Qian C, et al. Effects of voids on mechanical and thermal properties of the die attach solder layer used in high-power LED chip-scale packages[J]. IEEE Transactions on Components, Packaging and Manufacturing Technology, 2018, 8(7): 1254-1262.

[16] Mou Y, Wang H, Peng Y, et al. Enhanced heat dissipation of high-power light-emitting diodes by Cu nanoparticle paste[J]. IEEE Electron Device Letters, 2019, 40(6): 949-952.

[17] Peng J, Wang R C, Liu H S, et al. Mechanical reliability of transient liquid phase bonding of Au-Sn solder with Ni(Cu) substrates[J]. Journal of Materials Science, 2018, 29(1): 313-322.

[18] Yoon J W, Bae S, Lee B S, et al. Bonding of power device to ceramic substrate using Sn-coated Cu micro paste for high-temperature applications[J]. Applied Surface Science, 2020, 515: 146060.

[19] Shao H K, Wu A P, Bao Y D, et al. Novel transient liquid phase bonding through capillary action for high-temperature power devices packaging[J]. Materials Science and Engineering A, 2018, 724: 231-238.

[20] Tuo C J, Yao Z H, Liu W, et al. Fabrication and characteristics of Cu@Ag composite solder preform by electromagnetic compaction for power electronics[J]. Journal of Materials Processing Technology, 2021, 292: 117056.

[21] Chen T F, Siow K S. Comparing the mechanical and thermal-electrical properties of sintered copper (Cu) and sintered silver (Ag) joints[J]. Journal of Alloys and Compounds, 2021, 866: 158783.

[22] Liu Z Y, Cai J, Wang Q, et al. Modified pulse laser deposition of Ag nanostructure as intermediate for low temperature Cu-Cu bonding[J]. Applied Surface Science, 2018, 445: 16-23.

[23] 任辉, 张宏强, 王文淦, 等. 纳米金属颗粒焊膏低温烧结连接及其接头可靠性研究进展[J]. 中国激光, 2021, 48(8): 0802011.
Ren H, Zhang H Q, Wang W G, et al. Low-temperature sintering and joint reliability of metal nano-particle paste[J]. Chinese Journal of Lasers, 2021, 48(8): 0802011.

[24] Chen C T, Suganuma K. Large-scale ceramic-metal joining by nano-grained Ag particles paste sintering in low-temperature pressure-less conditions[J]. Scripta Materialia, 2021, 195: 113747.

[25] Yang F, Zhu W B, Wang X T, et al. Enhancement of high-temperature stability in sintered Ag joints on bare Cu substrates by inducing the transient liquid phase[J]. Materials Letters, 2021, 292: 129620.

[26] Liu J X, Mou Y, Peng Y, et al. Novel Cu-Ag composite nanoparticle paste for low temperature bonding[J]. Materials Letters, 2019, 248: 78-81.

[27] Xie Y J, Wang Y J, Mei Y H, et al. Rapid sintering of nano-Ag paste at low current to bond large area (>100 mm^2) power chips for electronics packaging[J]. Journal of Materials Processing Technology, 2018, 255: 644-649.

[28] 汤桦, 李强, 张启凡, 等. 领结型纳米银金属阵列对氮化镓基发光二极管光提取效率的影响[J]. 光学学报, 2021, 41(21): 2123001.

Tang H, Li Q, Zhang Q F, et al. Effect of bow Tie type silver metal array structure on light extraction efficiency of GaN-based light emitting diodes[J]. Acta Optica Sinica, 2021, 41(21): 2123001.

[29] 潘赛虎, 于航, 赵云平, 等. 金属纳米颗粒的导入对顶发射OLED光取出影响的FDTD模拟与研究[J]. 光学学报, 2022, 42(9): 0916001.
Pan S H, Yu H, Zhao Y P, et al. FDTD simulation and study on effect of metal nanoparticle introduction on light extraction of top-emitting OLED[J]. Acta Optica Sinica, 2022, 42(9): 0916001.

[30] Liu J X, Lei Z Y, Wang Q, et al. Fabrication of Sn-plated Cu foam for high-efficiency transient-liquid-phase bonding[J]. Materials Today Communications, 2022, 30: 103058.

[31] 唐燕如, 赵帝, 易学专, 等. 电流与温度对蓝光LED和白光LED发光性能的影响[J]. 中国激光, 2021, 48(21): 2103003.
Tang Y R, Zhao D, Yi X Z, et al. Current and temperature effects on luminescence properties of blue and white LEDs[J]. Chinese Journal of Lasers, 2021, 48(21): 2103003.

Thermal Resistance and Luminescence Performance of Nano-Silver Sintered Interface in High-Power LED

Liang Renli[1,2], Liu Jiaxin[3], Zhao Jiuzhou[4], Peng Yang[4], Wang Xinzhong[2**], Yang Jun[1*]

[1]*Shenzhen Institute for Advanced Study, University of Electronic Science and Technology of China, Shenzhen* 518110, *Guangdong, China*;

[2]*Information Technology Research Institute, Shenzhen Institute of Information Technology, Shenzhen* 518172, *Guangdong, China*;

[3]*School of Mechanical Science & Engineering, Huazhong University of Science and Technology, Wuhan* 430074, *Hubei, China*;

[4]*School of Aerospace Engineering, Huazhong University of Science and Technology, Wuhan* 430074, *Hubei, China*

Abstract

Objective Light emitting diodes (LEDs) are semiconductor light emitting devices based on the electroluminescence principle of p-n junction. Due to the advantages of high lighting efficiency, long life, environmental protection, energy saving, and compact structure, they have been widely used in the field of lighting and backlight display, such as road lighting, indoor lighting, automobile headlights, TV backlight, and mobile phone flash. With the increasing demand for lighting and display, LED technology is developing toward high power and high density. Therefore, luminescence performance has become an important indicator. Research shows that the luminescence performance of LEDs can be improved by employing the embedded ceramic circuit board technology and doping metals and other chemical compounds. However, the influence of LED heat dissipation on luminescence performance cannot be ignored. As the electro-optic conversion efficiency of LED is less than 60%, part of the input electric energy is converted into heat, and more heat is generated by the LED chip with the increase in the input power. For avoiding thermal damage to LED chips under high temperatures, it is significant to enhance the heat dissipation performance of LEDs, which can thereby improve the luminescence performance of high-power LEDs. This paper uses nano-silver paste for high-power LED packaging and systematically investigates the thermal resistance and luminescence performance of a nano-silver sintered interface in a high-power LED. Further, the paper analyzes the resistivity, bonding strength, and micromorphology of the nano-silver bonding layer at different sintering temperatures and compares the thermal resistance, junction temperature, and optical properties of LED devices sintered with nano-silver paste and Sn-Ag-Cu (SAC) solder.

Methods The nano-silver paste in this study is the silver paste after pressureless sintering. The chip used is a vertically packaged high-power blue LED chip with a direct plated copper (DPC) ceramic substrate, and the packaging substrate is a hexagonal copper substrate. Firstly, the chip and packaging substrate were cleaned by ultrasonic wave with acetone and anhydrous ethanol solution to remove the oil stain and impurities on the metal layer surface. Then, the nano-silver paste was coated on the hexagonal copper substrate by screen printing. The metal welding layer on the back of the DPC ceramic substrate containing chips was aligned to the copper substrate line layer and placed horizontally. After that, the LED samples were put into an oven for sintering to obtain the packaged high-power LED devices. Finally, the thickness of nano-silver films sintered at different temperatures was measured by a step profiler, and the sheet resistance of the sintered silver films was determined by a four-probe tester. The shear strengths of bonded joints were tested by a multifunctional shear force tester. The crystal structure of nano-silver paste after sintering was detected by X-ray diffraction. A scanning electron microscope (SEM) was used to observe the cross-sectional microstructure and fracture surface of the bonding

joints. The cross-sectional structure of the high-power LED was observed under an optical microscope. A thermal imaging system was used to record the surface operating temperature of the high-power LED. The junction temperature change and structural thermal resistance of the LED devices with different bonding materials were tested by a thermal resistance tester. In addition, a photoelectric analysis system was adopted to test the emission spectrum and light output power of LED samples.

Results and Discussions With the increase in sintering temperature from 180 ℃ to 240 ℃, the resistivity of the sintered samples decreases gradually, and the shear strength increases. High temperatures afford a large sintering driving force, which can accelerate the sintering and diffusion of nanoparticles. Therefore, nano-silver sintered at a high temperature has the characteristics of compactness and low resistivity. Nano-silver has better electrical conductivity and mechanical properties in the case of a higher sintering temperature (Fig. 2). The bonding layer of the high-power LED chip has a compact structure without holes and cracks. Moreover, the interfaces between the nano-silver layer and the upper and lower substrates exhibit good metallurgical bonding, which indicates that the LED sintered with nano-silver paste has excellent packaging quality (Fig. 3). The surface temperature of LED samples packaged with different bonding materials increases slowly with the increasing driving current. Compared with SAC305 solder, nano-silver has lower interface thermal resistance after sintering, which can improve the heat dissipation performance of LED devices and achieve lower operating temperature (Fig. 4). Due to the high thermal conductivity of nano-silver, the heat of the LED chip is dissipated faster (Fig. 5). The low interface thermal resistance of nano-silver is contributed to reducing the chip temperature and thereby lowering the junction temperature, which helps improve the reliability of LED devices (Fig. 6).

Conclusions In this paper, high-power LED devices are fabricated by nano-silver sintering technology, and the interface thermal resistance and luminescence performance of the bonding layer are emphatically investigated. The experimental results illustrate that with the increase in the sintering temperature, the resistivity of nano-silver decreases, and the bonding strength of joints increases. The interface of the nano-silver sintered LED bonding layer is compact and crack-free, forming good metallurgical bonding. The LED sample sintered with nano-silver paste has a lower working temperature and lower total thermal resistance than that sintered with SAC305 solder, and the interface thermal resistance of the LED sample sintered with SAC305 solder is 8.9% higher than that of the nano-silver sintered one. These findings indicate that nano-silver has higher thermal conductivity and better heat dissipation performance. In addition, the luminous efficiency of the aged LED sample sintered with nano-silver paste is invariably higher than that of the sample sintered with SAC305 solder at different input currents.

Key words materials; high-power LED; opto-thermal performance; luminescence stability; nano-silver sintering; interface thermal resistance